ELSEVIER

Biophysical Chemistry 119 (2006) 282 – 294

Biophysical Chemistry

http://www.elsevier.com/locate/biophyschem

The Na^+ binding channel of human coagulation proteases: Novel insights on the structure and allosteric modulation revealed by molecular surface analysis

Floriano P. Silva Jr. [a,b,*], Octávio A.C. Antunes [b], Ricardo B. de Alencastro [b], Salvatore G. De Simone [a,c]

[a] *Laboratório de Bioquímica de Proteínas e Peptídeos, Departamento de Bioquímica e Biologia Molecular, Instituto Oswaldo Cruz, Fundação Oswaldo Cruz, 21045-900, Rio de Janeiro, RJ, Brazil*

[b] *Departamento de Química Orgânica, Instituto de Química, Universidade Federal do Rio de Janeiro, Cidade Universitária, 21949-900, Rio de Janeiro, RJ, Brazil*

[c] *Departamento de Biologia Celular e Molecular, Instituto de Biologia, Universidade Federal Fluminense, 24001-970, Niterói, RJ, Brazil*

Received 21 July 2005; received in revised form 30 September 2005; accepted 1 October 2005
Available online 9 November 2005

Abstract

Thrombovascular diseases result from imbalanced haemostasis and comprise important health problems in the aging population worldwide. The activity of enzymes pertaining to the coagulation cascade of mammalians exhibit several control mechanisms in order to maintain a proper balance between bleeding and thrombosis. For instance, human coagulation serine proteases carrying a F225 or Y225 are allosteric modulated by the binding of Na^+ in a water-filled channel connected to the primary specificity pocket (S1 subsite) of these enzymes. We have characterized the structure, topography and lipophilicity of this channel in the ligand-free fast (sodium-bound) and slow (sodium-free) forms of thrombin, in the sole available structure of activated protein C and in several structures of the coagulation factors VIIa, IXa and Xa, differing in the nature of the bound inhibitor and in the occupancy of exosite-I as well as the Ca^{2+} and Na^+ binding sites. Opposite to thrombin, the aqueous channels in all other coagulation enzymes sheltering a Na^+ binding site do not have an aperture on the enzyme surface opposite to the S1 subsite entrance. In these enzymes, the lack of the three-residue insertion in loop 1 (183–189) as found in thrombin allied to compensatory mutations in the positions 187–185 and 222 effects a constriction in the water-filled channel that ends up by segregating the ion binding site from the S1 subsite. We also disclosed major topographical changes on the thrombin's surface upon sodium release and transition to the slow form that culminate in the narrowing of the S1 subsite entrance and, strikingly, in the loss of communication between the primary specificity pocket and the exosite-I. Such observation is in accordance with existing experimental data demonstrating thermodynamic linkage between these distant regions on the thrombin surface. Conformational changes in F34, L40, R73 and T74 were the main responsible for this effect. A path by which these changes in the vicinity of exosite-I could be transmitted to the S1 subsite and, consequently, to the sodium binding site is proposed.

Keywords: Allostery; Na^+ binding; Molecular modeling; Thrombin; Coagulation factors; Serine proteases

1. Introduction

The physiologic response to a vascular lesion entails a number of sequential enzymatic steps catalyzed by distinct serine proteases, known as the coagulation cascade [1–3]. Vein or artery rupture triggers the formation of a calcium- and phospholipid-dependent complex between the plasmatic protein known as activated factor VII (FVIIa) and tissue factor (TF). In the next step, the tenase complex activates factor X and the resultant activated factor X (FXa) subsequently associates with activated factor V (FVa) on the surface of TF-bearing cells to form a prothrombinase complex. As the name suggests, the later converts the inactive circulating thrombin precursor, prothrombin, into its active form. Significantly, the tenase complex is also able to process a small amount of factor IX and the activated factor IX (FIXa) can diffuse to the surface of lesion-recruited platelets and activate FX with out being significantly

* Corresponding author. Laboratório de Bioquímica de Proteínas e Peptídeos, Departamento de Bioquímica e Biologia Molecular, Instituto Oswaldo Cruz, Fundação Oswaldo Cruz, 21045-900, Rio de Janeiro, RJ, Brazil. Tel.: +55 21 3865 8157; fax: +55 21 2590 3495.

E-mail address: floriano@ioc.fiocruz.br (F.P. Silva).

0301-4622/$ - see front matter © 2005 Elsevier B.V. All rights reserved.
doi:10.1016/j.bpc.2005.10.001

inhibited by TFPI or ATIII. In the final step of the coagulation cascade, the release of fibrinopeptides A and B by the action of thrombin over fibrinogen α and β chains, respectively, leads to the formation of fibrin monomers. An important regulatory pathway of the coagulation process results from the inactivation of factors Va and VIIIa by activated Protein C (aPC). The formation of the later is catalyzed by a complex between thrombin and thrombomodulin, a transmembrane protein from the endothelium.

Thrombin is a multifunctional protease, central to the coagulation process in mammals and other vertebrates. As such, thrombin must be under very tight control and consequently must interact with different substrates and molecular modulators. This diversity of functional interactions is also present in other serine proteases operating in the coagulation cascade, such as aPC and factors VIIa, IXa and Xa. Overall, efficiency of the coagulation system requires a rapid and localized response at the injury site that can be readily terminated. This is accomplished through a plethora of regulatory mechanisms among which sodium mediated allostery has emerged as the simplest and most intriguing [4]. The physiological role of sodium as a thrombin allosteric modulator was disclosed short after the characterization of the Na^+ dependent conformational change and activation of the enzyme was reported [5]. The fast form that is generated after Na^+ binding is considered procoagulant primarily because it cleaves fibrinogen with higher specificity than Protein C. Oppositely, the Na^+-free, slow form, is thought to be anticoagulant due to its higher specificity for Protein C in comparison to fibrinogen.

The activating effects of Na^+ over the hydrolytic activities of the coagulation proteases, FXa, thrombin and aPC, has been known for many years [6–8]. The coagulation factors FVIIa and FIXa are suspected to shelter a Na^+ binding site based upon the Dang and Di Cera's rule [9]. This rule was elaborated after the canonical thrombin Na^+ binding site (Fig. 1) was identified crystallographically through rubidium substitution [5,10]. It states that serine proteases of the chymotrypsin family (clan S1A) carrying a phenylalanine or a tyrosine residue at position 225 can properly provide a Na^+ binding site whereas family members presenting P225 cannot. Indeed, it was demonstrated that FIXa displays a 4-fold enhancement in specificity for synthetic amide substrates upon Na^+ addition to the reaction media [11].

The specificity of coagulation serine proteases is primarily dictated by the complementary interactions between the major pocket in the substrate binding cleft (the S1 subsite) and the side chain of the residue N-terminal to the scissile bond (P1 residue). Nonetheless, these enzymes display on their surfaces other sites involved in substrate recognition such as the exosite-I in thrombin and the Ca^{2+} binding site found in aPC and coagulation factors VIIa, IXa and Xa. These sites are distributed in analogous regions of the serine protease COOH-terminal domain. Exosite-I is delineated by loops

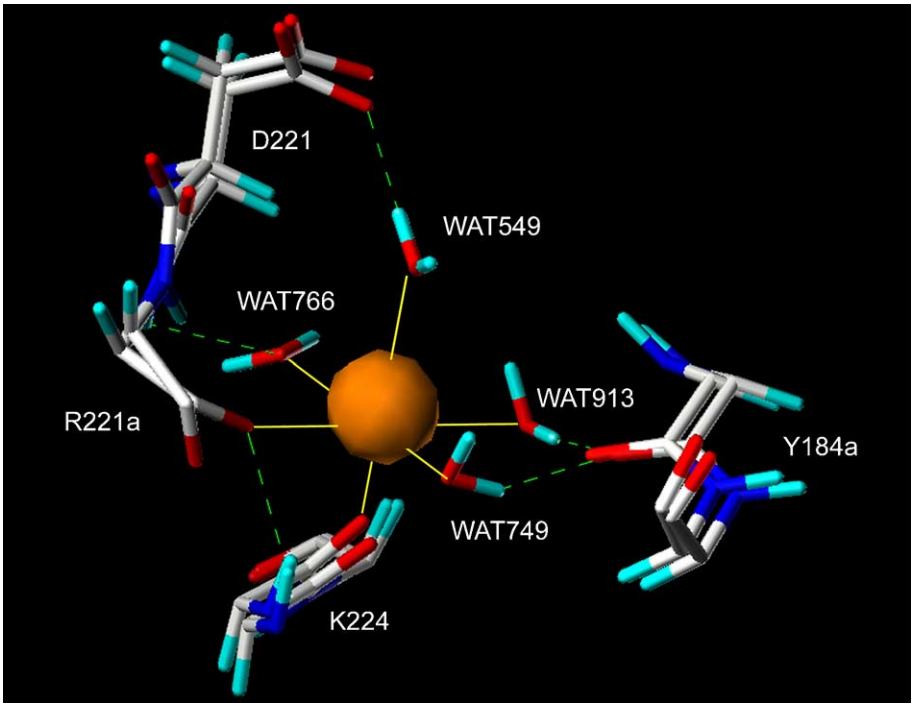

Fig. 1. Comparison of the Na^+ coordinating residues conformations in thrombin fast and slow forms. The Na^+ ion is plotted as an orange van der Waals sphere while protein residues are depicted as CPK-colored capped sticks. For the fast form, water molecules coordinating Na^+ are shown along with hydrogen bonding interactions (green dashed lines; 2 dashes per angstrom) and coordination bonds (yellow lines), which is composed of the carbonyl O atoms of residues 224 and 221a and four water molecules in thrombin or in the case of aPC and FXa by the carbonyl oxygen atoms of residues 185, 184a, 224 and 221a along with two water molecules. The site architecture is largely maintained upon sodium release by the thrombin fast form (pdb 1SG8) and transition to the slow form (pdb 1SGI). One important exception is the loop 1 backbone whose change in conformation culminating at residue R221a (depicted by deviations of 41.4° and 31.9° in ϕ and ψ torsion angles, respectively) moves the carbonyl oxygen atom in the slow form almost 1.0 Å away from its position relative to the fast form.

74–80 as well as part of the adjoining strands (residues 81–82 and 85–87) and is responsible for mediating essential interactions with the thrombin's natural pro-coagulant substrate, fibrinogen [12], as well as for providing a binding site for thrombomodulin [13]. The calcium binding site is formed by structures in the 70–80 loop and is typified by the one first described in trypsin [14]. This site is functionally relevant because it has been shown that a Ca^{2+} ion is required for efficient activation of Protein C by the thrombin–thrombomodulin complex [15,16] while it has also been shown to be a necessary co-factor or to significantly enhance the catalytic activities of factors VIIa and Xa, respectively [17,18].

The unique monovalent metal binding site in sodium activating coagulation enzymes is inserted in a cavity nearly opposite to the entrance of the S1 subsite and can be traced to a region located 15–16 Å away from the catalytic triad. In thrombin and FXa, a network of water molecules has been described to link the Na^+ binding site to the S1 subsite [10]. Ala-scanning studies accompanied by the structural elucidation of carefully crystallized inhibitor-free R77aA thrombin mutants in the Na^+ bound and unbound states revealed that very subtle and localized conformational changes in loops 1 (184–189) and 2 (221–225) underlie sodium mediated activation [19]. Slow-fast transition results from the formation of the R187:D222 ionic pair allied to the optimal reorientation of D189 and to the significant changes in E192 orientation [20]. All of these changes are coupled to the rearrangement in the water network that connects the cation to S195 in the catalytic site. Interestingly enough, experimental data support an energetic linkage between exosite-I, the Na^+ binding site and the active site [13,21], although a definitive structural basis for this connection is still missing. Similarly, thermodynamic or functional linkage between the S1 subsite, and the Na^+ and Ca^{2+} binding sites has been shown for aPC, FIXa and FXa [22–24].

Recently, using computer-aided molecular surface analysis (CaMSA) our group evidenced the shape of the hydrophilic channel connecting the sodium binding site to the S1 subsite [25]. The importance of shape complementarity in biomolecular complex formation has been fostered by the knowledge accumulated through years studying molecular recognition processes [26]. Hence, in giving the opportunity to begin examining extensive Ala-scanning and other functional data at a more intuitive level, i.e., the molecular surface, we have envisaged that CaMSA would arose as a powerful methodology to bring novel insights on the mechanisms behind Na^+ recognition and allostery.

Here we report the application of CaMSA to the study of the sodium binding channel shapes of the human coagulation proteases thrombin, factors VIIa, IXa, Xa and aPC. As Na^+ ions are rarely directly identified in crystallographic studies many of the structures reported in the past for coagulation proteases were not characterized as to their Na^+ binding state. Therefore, for the properly unbiased application of CaMSA methodology we had to carefully screen these structures for the presence of an unnoted Na^+ ion as well as other allosteric effectors, such as Ca^{2+} and exosite-I ligands. In addition to the comparisons of the channel shape features among the enzymes we also describe, for the first time, an analysis of the Na^+ binding sites in factors VIIa and IXa. Except for thrombin, no other enzyme structure was available in both the fast and slow forms. Hence, the application of CaMSA to the characterization of the slow-fast transition had to be limited to thrombin.

2. Experimental

2.1. Structures and characterization of sodium and calcium binding states

All molecular manipulations and calculations described in this section were performed in Sybyl v6.8 (Tripos Inc., St. Louis, MO). Structures for thrombin fast and slow forms, aPC and factors VIIa, IXa and Xa were retrieved from the PDB. The structures of aPC and factors VIIa, IXa and Xa were also searched for Ca^{2+} ions whenever these were not reported in the coordinate files. The binding sites for Ca^{2+} were characterized with respect to residues possibly involved in the coordination sphere through the aid of molecular graphics. Whenever it was not explicitly stated in the coordinate files, the presence of sodium ions that would have been incorrectly assigned to water oxygen atoms was investigated with the program WASP [27]. The program WASP was chosen for that purpose because it pertains to a class of methods based on valence calculations, which proved to be very accurate [27], and because it is readily available.

2.2. Modeling of the hydrogen bonding network in the S1 subsite and sodium binding water channel

For the calculations, only bound water molecules, belonging to the S1 subsite or to the sodium binding water channel, were retained, other ligands, except for Na^+, were deleted from the coordinate files and hydrogen atoms were added. In order to efficiently account for hydrogen bonding interactions in the region around the S1 subsite and the sodium binding water channel we have employed the ANNEAL command with help of the "minimize subset" dialog of the Sybyl v6.8 graphical interface. The Tripos force-field was used with a non-bonded cutoff of 8.0 Å and Kollman all-atoms charges were assigned. A gradient inferior to 0.05 kcal/mol Å was used as the termination criterion. The minimization protocol, where only hydrogen atoms were allowed to move, consisted of two phases: initially, a maximum of 20 simplex steps followed by a hundred steps of steepest descent was employed; then, 1000 steps of conjugated gradients were performed.

2.3. Computer-aided molecular surface analysis (CaMSA)

As first described [25], CaMSA methodology essentially combines calculation of Connolly channel surfaces [28–30] with arbitrary indexes of cavity lipophilicity based on lipophilic molecular surface potentials [31]. Briefly, structures were minimized as stated in the above section and had their

ligands (if any) and water molecules deleted, followed by addition of all hydrogen atoms. Addition of all polar and non-polar hydrogen atoms is a requirement for the correct assignment of atomic lipophilic potentials as they were originally derived [31]. Then, using MOLCAD program in Sybyl v6.8 (Tripos Inc., St. Louis), fast Connolly channel surfaces were calculated and the lipophilic potential mapped over the cavity surface. Lipophilic potential ranges were adjusted to −0.20 to +0.10 and areas under low (−0.20 to −0.10), medium (−0.10 to 0.00) and high (0.00 to +0.10) lipophilicity were mapped.

3. Results

3.1. Na^+ binding states and coordination partners in factors VIIa and IXa

The structures of coagulation serine proteases used in this study were selected to reflect different binding states for the active and allosteric sites (Na^+, Ca^{2+} and inhibitors). The 17 structures (2 thrombins, 8 FXas, 1 aPC, 2 FIXas and 4 FVIIas) are listed in Table 1. Characterization of Na^+ binding states required careful inspection of solvent molecules in order to determine if a sodium atom was not confounded with isoelectronic water oxygen during crystallographic refinement. In the case of factors VIIa and Xa, where several coordinate files were screened for the presence of Na^+, we selected a number of structures differing in crystallization conditions, space group and cocrystallized inhibitor. This was performed in order to have a proper representation of the molecular surface, discarding possible artifacts (Table 1).

To the best of our knowledge, the Na^+ binding sites in coagulation factors VIIa and IXa have not been described yet. Therefore, we embraced the characterization of Na^+ binding partners in these proteases. The conformations of residues involved in Na^+ coordination in thrombin (pdb 1SG8) and FXa (typified by pdb 1MQY) were compared with the conformations of residues at the structurally equivalent positions in FVIIa (embodied by pdb 1CVW) and FIXa (exemplified by pdb 1RFN) structures (Fig. 2). Contrary to the available inhibitor-free FVIIa structure (pdb 1KLJ), the benzamidine inhibited FVIIa structure (pdb 1CVW) showed a water molecule (WAT605) near to the Na^+ position in thrombin (1.63 Å) and FXa (1.21 Å). The WASP program probably did not recognized this water molecule as a candidate for a sodium ion because of its unfilled valence. At least one of the water ligands coordinating the monovalent cation in thrombin (WAT549) or FXa (WAT729) was missing in the FVIIa structure analyzed (water site 2, WAT-2, in Fig. 2). The conformations of FVIIa residues in loop 1 are more similar to these displayed by FXa than to the residues in the equivalent thrombin segment. This observation supports the presence of a Na^+ binding site in FVIIa, which is similar to FXa, where two of the water molecules coordinating Na^+ in thrombin are replaced by two carbonyls from residues in loop 1. Hence, in FVIIa, the metal coordination partners probably are the backbone carbonyls of Y184 (Y185 in FXa 1MQY) and S185 (D185a in FXa 1MQY) in loop 1, T221 (R221a in thrombin 1SG8 and R222 in FXa 1MQY) and K224 in loop 2, and the oxygen atoms of solvent molecules positioned at water site 1 (WAT-1) and WAT-2 (Fig. 2).

As can be perceived from Fig. 2, FIXa presented a poor superposition in loops 1 and 2 either with FXa or thrombin fast form. The highest RMSD occurs in positions 185 (185a in

Table 1
Analysis of lipophilic potentials for the S1 subsite containing cavity in sodium binding coagulation enzymes

Structures					Area of S1 subsite containing cavity				
Enzyme	PDB code	Ligands present?			Total[a] (Å^2)	Lipophilic potential[b] (%)			
		Na^+ (water)	Ca^{2+}	Inhibitor		Low	Medium	High	Total lipophilic[c]
Thrombin	1SG8	Y (N.A.[d])	–	N	919.2	11.0	77.9	11.1	89.0
	1SGI	N (N.A.)	–	N	792.7	13.5	73.7	12.8	86.5
FXa	1KIG	N (N.A.)	N	Y, AS[e]	1080.7	7.9	84.0	8.1	92.1
	1HCG	Y (583)	N	Y[f]	463.9	2.7	91.0	6.4	97.4
	1MQ5	Y (733)	Y	Y, AS	489.8	9.1	70.9	20.0	90.9
	1NFY	Y (24)	Y	Y, AS	434.4	8.9	85.4	5.8	91.1
	1KSN	Y (11)	Y	Y, AS	518.9	6.4	79.6	14.0	93.6
	1G2L	Y (500)	Y	Y, AS	582.4	7.6	75.1	17.3	92.4
	1IQG	Y (577)	Y	Y, AS	375.7	11.9	82.9	5.2	88.1
	1XKA	Y (680)	Y	Y, AS	409.6	11.3	73.8	15.0	88.8
aPC	1AUT	N (N.A.)	N	Y, AS	374.4	17.9	81.6	0.4	82.0
FIXa	1PFX	N (N.A.)	N	Y, AS	421.5	6.6	88.9	4.5	93.4
	1RFN	N (N.A.)	Y	Y, AS	330.0	20.7	79.1	0.3	79.4
FVIIa	1CVW	N (N.A.)	Y	Y, AS	290.0	34.7	65.3	0.0	65.3
	1DAN	N (N.A.)	Y	Y, AS[g]	300.8	32.6	67.4	0.0	67.4
	1DVA	N (N.A.)	Y	Y[h]	281.6	32.9	67.1	0.0	67.1
	1KLJ	N (N.A.)	Y	N	336.6	24.1	75.9	0.0	75.9

[a]Areas calculated from the total cavity detected by the MOLCAD module in Sybyl v.6.8, Tripos Inc. [b]Areas under the following lipophilicity ranges — low: −0.20 to −0.10; medium: −0.10 to 0.00 and high: 0.00 to 0.10. Percentages are expressed in relation to total cavity area. [c]Calculated from the sum of areas within medium and high lipophilic potential. [d]Not applicable. [e]active-site bound. [f]Although this structure has no added inhibitor the COOH-terminal of the FXa A-chain interacts in a substrate-like manner with the active site of a neighboring FXa molecule. [g]Bound to soluble tissue factor. [h]Peptide exosite inhibitor.

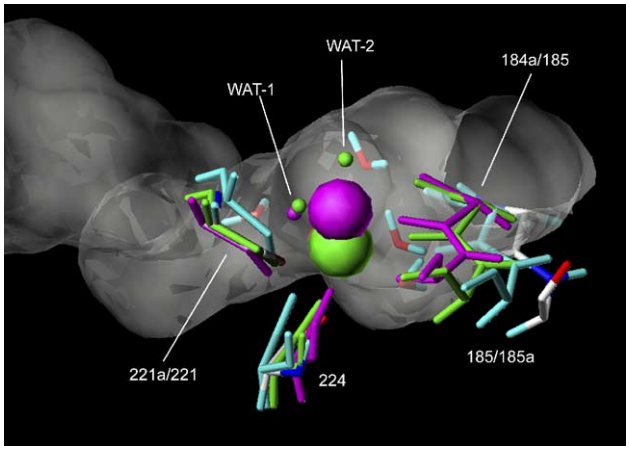

Fig. 2. Characterization of Na^+ binding sites in coagulation factors VIIa and IXa. The putative Na^+ binding partners in FVIIa (pdb 1CVW) and FIXa (pdb 1RFN) were compared with the known metal ligands in thrombin fast form and FXa (pdb 1MQY). Proteins are color-coded: thrombin — CPK, FXa — green, FVIIa — magenta and FIXa — cyan. Known (thrombin and FXa) and putative (FVIIa) sodium ions are shown as van der Waals spheres. Thrombin water molecules are shown with hydrogen atoms while waters pertaining to FXa or FVIIa are depicted only by their oxygen atoms. The thrombin channel surface is shown in gray and had its surface rendered transparent.

FXa) and 224. These particular conformations would be compatible either with flexibility in Na^+ binding site architecture, in similar fashion to aPC, or with an alternative sodium binding site in FIXa. This site would be a hybrid in which features of the Na^+ binding sites in thrombin and FIXa would be joined in a single framework. In particular, it would be possible that a water molecule bound to the carbonyl of H185 would occupy one of Na^+ coordination sites in FIXa, analogously to thrombin. The remaining ligands in the sodium coordination sphere would be represented by the carbonyl oxygen atoms of F184a, M221a and K224 and water molecules in WAT-1 and WAT-2.

3.2. CaMSA of the S1 subsite and the sodium binding water channel

As employed in the original CaMSA methodology [25], lipophilic potentials were mapped on the channel surfaces of the coagulation enzymes. It was shown that lipophilic potentials could be directly correlated to the binding affinities of trypsin-like proteases for S1 ligands. In this sense, we hypothesized that the conformational changes associated with the slow-fast transition and the resulting increase in catalytic rate could be related to an increase in surface lipophilic potential. Calculated areas for the different ranges of cavity lipophilic potentials for the sodium binding coagulation enzymes are listed in Table 1. There was a small increase in the lipophilic area of thrombin upon sodium binding. Similarly, there was a slight tendency of Ca^{2+}-free enzymes to present higher lipophilicity on their channel surfaces. These observation may reflect changes on the exposure of polar groups on the protein surface upon binding of Na^+ or Ca^{2+}.

Differences in solvent accessible surface (SAS) areas of the analyzed structures were also observed (Table 1) and were related to the shape of the cavities depicted in Fig. 3. The cavities in FVIIa, FIXa and aPC are very similar and are essentially restricted to the S1 subsite and the adjoining hydrophilic channel linking the Na^+ binding site to the primary specificity pocket. Data in Table 1 also show a significantly higher SAS for most human FXa structures (pdb codes 1HCG, 1MQY, 1KSN and 1G2L) in relation to aPC and factors VIIa and IXa. This is a result of an extension of the cavity surface that reaches the regions corresponding to the S3 and S2 subsites.

Employing the same analysis to the catalytic domain of bovine FXa (pdb id 1KIG) a very complex surface is obtained. Differently from all human FXa structures, it involves the S1 subsite and the adjoining water channel as well as projections that reach almost all of the substrate binding cleft, from the non-primed (S2–S4) to the primed subsites (S1′–S3′) near the Ca^{2+} binding site (not shown). The high sequence similarity (84.5% in 233 residues) between the orthologous bovine and human enzymes precludes the use of divergence in primary structure as an argument to explain these drastic differences in topographical features. The 3D structure of the bovine enzyme was reported without bound Ca^{2+} and Na^+ as well as any solvent molecules [32]. Perhaps, association of these observa-

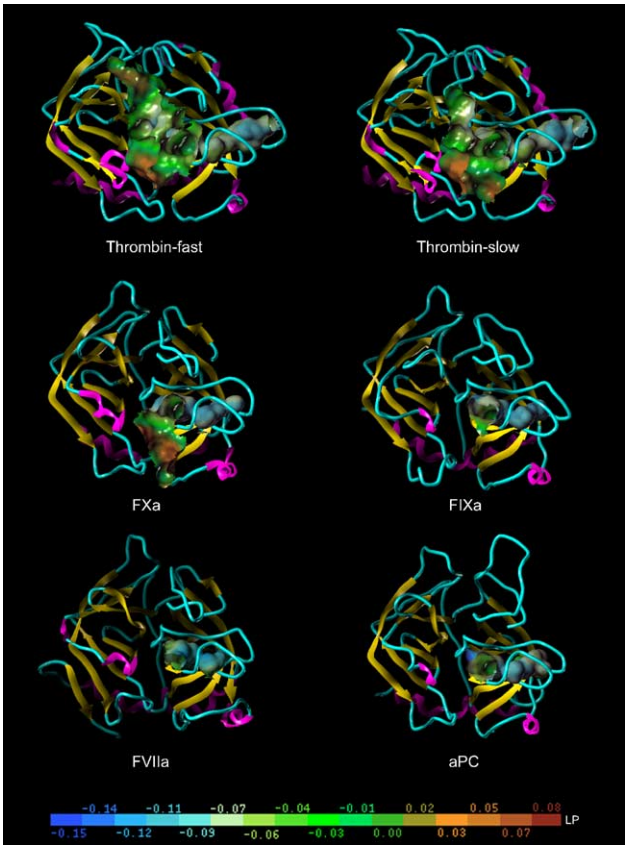

Fig. 3. General topography and lipophilicity of the major channels/cavities in human coagulation enzymes bearing a sodium binding site in the catalytic domain. On the bottom is shown the color-code for the lipophilic potential range: lipophilicity grows from bluish (hydrophilic) to brownish (lipophilic) shades. Protein secondary structure is color-coded and represented as ribbons.

tions in terms of the presence or absence of such allosteric modulators could provide an explanation to the markedly distinct topographical features of the bovine FXa surface as a consequence of global conformational changes in the enzyme structure by effect of Ca^{2+} release.

A comparison of the structures surrounding the divalent metal binding sites in the FXa orthologues disclosed significant conformational changes possibly related to the release of the Ca^{2+} ion. First of all, it is important to note that G79 in the human enzyme is substituted for N79 in the bovine FXa. This gives a priori justification for the changes in the backbone conformation of the calcium binding loop, particularly in the segment 75–78. Nevertheless, there is a drastic reversal in the direction of the E80 carboxylate group, which points toward the solvent in the Ca^{2+}-free bovine enzyme. Whether the observed displacement in the loop engaged in Ca^{2+} binding (residues 70–80) would cause the abrogation of the metal binding site in bovine FXa is not certain but the reorientation in E80 side chain would surely be related to the absence of a bound Ca^{2+} ion. In fact, the human FXa structure reported without Ca^{2+} in the catalytic domain (pdb id 1HCG) the E80 side chain is in a conformation intermediary between the solvent exposed, as observed in the bovine enzyme, and the one involved in calcium coordination, as in all other Ca^{2+}-bound FXa catalytic domain structures.

It is clear from the data in Table 1 and inspection of Fig. 3 that both thrombin allosteric forms have a larger cavity SAS than the other coagulation enzymes (with exception of bovine FXa). Distinctly from aPC and human factors VIIa, IXa and Xa, the cavity surfaces for thrombin allosteric forms entail not only the S1 subsite and the water channel but also a great part of the substrate binding cleft, from S3 to S3′. But, more importantly, the free thrombin fast form presents a continuous surface connecting the sodium binding water channel and the S1 subsite to the region corresponding to the prime-side subsites (S1′–S4′) and exosite-I, a feature not observed in the slow form (Fig. 4). Since the connection with the exosite-I is lost in the slow form, a marked shortening of the cavity SAS is observed. This fact is accompanied by a pronounced narrowing of the entrance to the S1 subsite in the slow form.

Another feature of the surfaces compared in Fig. 3 is that, except for thrombin, the water channels in all other sodium binding coagulation proteases do not open to the enzyme surface. It is clear from the alignment of Na^{+}-regulated coagulation enzymes in Fig. 5 that the unique three-residue insertion in the thrombin loop 184–189 (loop 1) leads to the aperture in the channel extremity opposite to the S1 subsite. Loop 1 and loop 2 support most of the architecture of the S1 subsite and the adjoining water channel. We have made a comparison of the backbone conformations for loop 1 in thrombin with the other coagulation proteases bearing a Na^{+} binding site (Fig. 6). It clearly shows that this loop in the later enzymes is dislocated toward the channel lumen imposing a constriction that ends up by occluding the communication with the external part of the enzyme surface (e.g., FXa in Fig. 6A and C). In general, the maximal displacement occurs in position 222, e.g., 1.6 Å in the Cα positions in aPC and thrombin compared to 1.14 Å RMSD in the whole loop (Fig. 6B).

3.3. Mapping of residues involved in topographical changes in thrombin surface upon Na^{+}-mediated allosteric transition

Fig. 7 shows in detail some important residues responsible for the channel architecture and the underlying water network for thrombin slow and fast forms. As reported above, sodium release results in the narrowing of the S1 subsite entrance in thrombin. Inspection of the structures for the thrombin fast and slow forms revealed that a conformational change in E192 side chain is responsible for this effect (compare panels A and B in Fig. 7). The rearrangement in the water network associated with the movement in E192 side chain is also evident. Comparison of the panels in Fig. 7 also reveals that the rupture in the double hydrogen-bonding interaction between R187 and D222 upon transition of the fast to the slow form has virtually no effect over the channel shape near its aperture opposite to the S1 subsite.

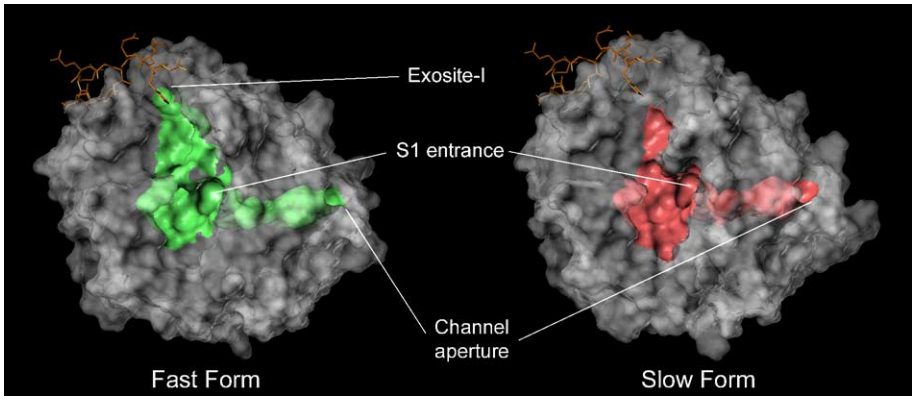

Fig. 4. Coverage of the cavity bearing the Na^{+} binding channel in thrombin fast and slow forms. Solvent accessible surfaces (1.4 Å probe) for the whole molecules were made transparent to turn evident the range of the cavity bearing the water channel and specificity pockets. An exosite-I ligand, *N*-acetylhirudin[53–64]-Tyr63-sulfate (orange sticks), was transposed from the PDB structure 1HAH in order to locate this site on the thrombin surface.

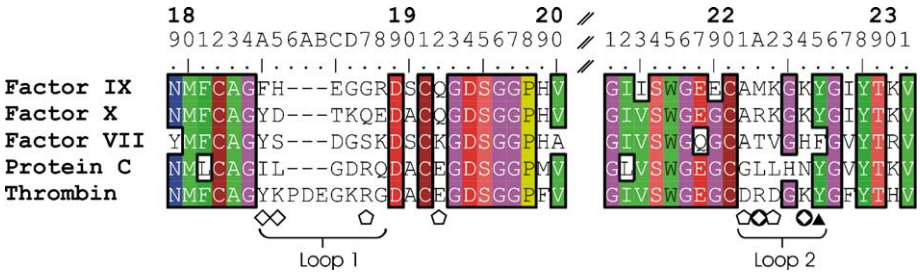

Fig. 5. Multiple sequence alignment of human coagulation enzymes in the segments involved in the architecture of the sodium binding site. Loops 1 and 2 are identified along with residues responsible for Na^+ coordination in FXa (lozenges) or thrombin (solid circles) and residues important for the Na^+ binding channel structure (pentagons and solid triangle).

Upon thrombin fast–slow transition, the continuity in surface linking the S1 subsite to the exosite-I region is lost. In order to better analyze structures in exosite-I, *N*-acetylhirudin[53–64]-Tyr63-sulfate (orange sticks) was copied from its bound conformation in the thrombin structure 1HAH and docked by superposition in the fast form structure. Inspection of the modeled complex, in the region underlying the surface near exosite-I, where the communication is abrogated, indicated changes in the conformation of some residues upon comparison of fast and slow thrombin structures. Part of the thrombin fast form secondary structure elements and intervening loops (beta-sheet comprising strand segments 32–36, 38–40 and 63–67, and loop 73–75) that define this "hot region" and are in contact distance (<4.0 Å) from the modeled exosite-I ligand is shown as color-coded ribbons in Fig. 8A. The hot region is located in the exosite-I periphery and is comprised of F34, Q38, L40, R73 and T74 (Fig. 8B). For instance, residue L40 undergoes rotations in the $\chi 1$ and $\chi 2$ dihedral angles that place the isopropyl moiety nearer to the interior of the cavity (Fig. 8C). This conformational change contributes to the rupture of the communication between the S1 subsite and the exosite-I.

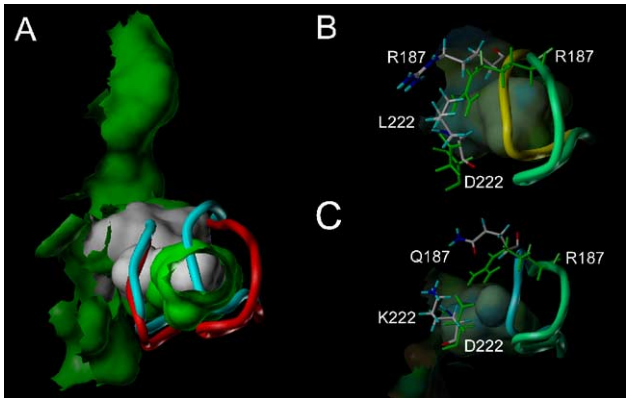

Fig. 6. Comparison of loop 1 conformation in selected human coagulation enzymes. A-Superposition of Na^+ binding channels along with loops 1 and 2 in thrombin fast form (pdb id 1SG8; green surface and red tubes) and FXa (pdb id 1MQY; white surface and cyan tubes). B-Superposition between loop 1 in aPC (pdb id 1AUT; yellow tube) and thrombin fast form (green tube). Residues responsible for stabilizing the tip of the channel are shown in sticks, CPK-colored for aPC and green for thrombin. C-Superposition between loop 1 in FXa (pdb id 1MQY; cyan tube) and thrombin fast form (green tube). Residues are colored in CPK for FXa and green for thrombin.

Similarly, it can be perceived from Fig. 8C that the side chains of residues F34, Q38, R73 and T74 experience considerable repositioning, which culminates in the blockage of the continuity on the surface connecting the S1 subsite to the exosite-I.

The fact that the set of residues responsible for disrupting the surface linkage between S1 subsite and exosite-I is located around 25 Å away from the sodium atom raises the question of which structural elements are connecting these residues to the sodium binding site and the S1 subsite. W141, G193 and nearby residues (e.g., N143 and Q151) that are in contact distance (4.0 Å) to the hot region emerged as interesting candidates for this role (Fig. 9). Furthermore, two water molecules located at the point of differentiation between cavities of the fast and slow thrombin forms can form hydrogen bonds to the amide carbonyls in Q151 and N143 side chains, and to the W141 backbone. These bound waters are exclusive of the fast thrombin form. Modeling of the hydrogen bonding network that connects bound water molecules in thrombin structure confirmed this. In fact, one of the above mentioned water molecules donates a hydrogen bond to the amide carbonyl of N143, which in turn, accepts a hydrogen bond from the other water molecule. The later also participate in hydrogen bonding with W141 backbone carbonyl. This interaction network could be important for connecting events in the exosite-I periphery originating in T74 and passing on through R73, W141, N143 to G193 in the classical chymotrypsin-like serine protease oxyanion binding hole.

4. Discussion

4.1. Loop 1 may be responsible for Na^+ specificity in human coagulation proteases

Our comparative analysis of the monovalent cation binding sites in FVIIa and FIXa along with the other previously described sites in thrombin, FXa and aPC gives a hint about the striking efficacy of the Dang and Di Cera's rule. We also compared the sodium binding site in the, public available, Na^+-free aPC structure (pdb id 1AUT) with the description of the Na^+ coordinating sphere in the aPC structure determined before [22]. In its sodium-free form, the backbones of residues 184a and 185 superpose very well with the equivalent thrombin

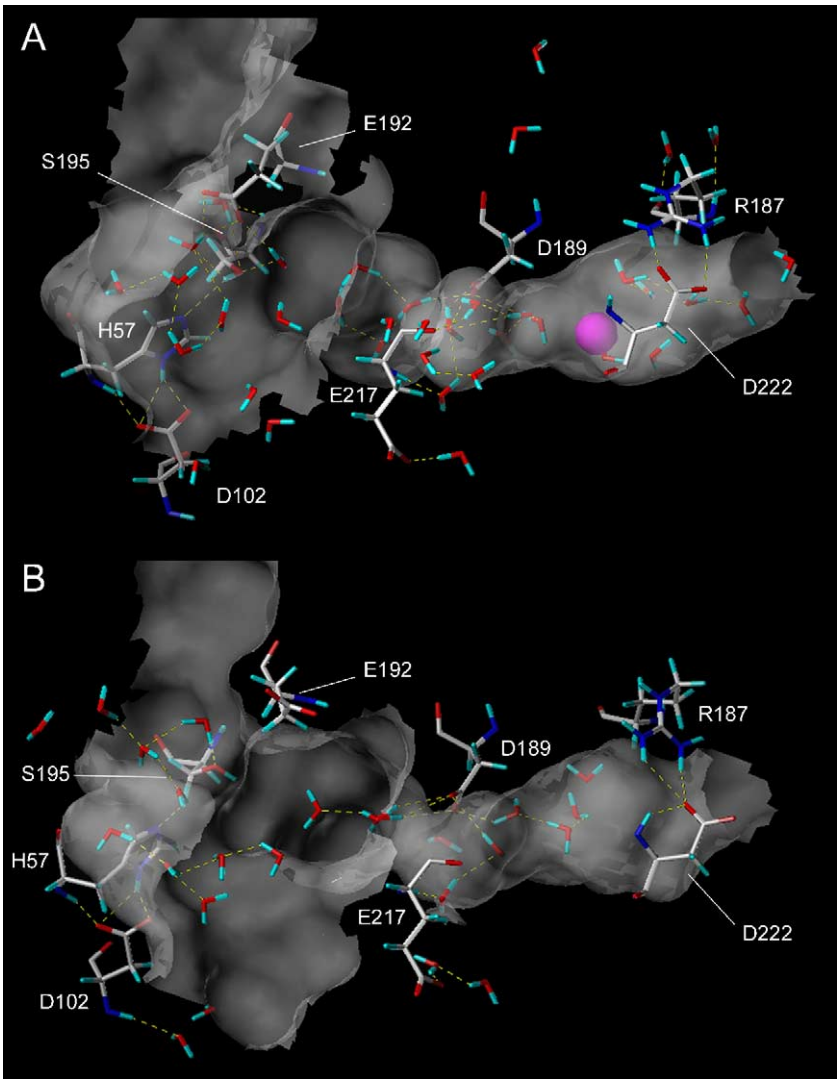

Fig. 7. Comparison of the channel shape in the fast and slow forms of thrombin. Some important residues responsible for the channel structure are identified in the figure along with bound water molecules pertaining to the hydrogen-bonded network surrounding the S1 subsite and sodium binding site. Note E192 orientation in the ligand-free slow and fast forms of thrombin resulting in the narrowing of S1 subsite entrance. The breakage of R187:D222 salt bridge in the slow form produces no observable difference in the subjacent region of the channel surface, as compared to the fast form. Also, observe the different pattern of hydrogen bonding interactions (dashed yellow lines) involving the water molecules associated with the slow–fast transition.

segment (not shown). Consequently, in the Na^+-free aPC, one of the former Na^+ ligands in the structure reported by Schmidt et al. has its carbonyl oriented away from the Na^+ ion, preventing its role as a sodium coordination partner [22]. This suggests a high level of flexibility in loop 1 that seems to be unique to aPC.

Indeed, comparison of the loop 1 conformation in all coagulation proteases thought to bind Na^+ showed that its flexibility is considerably higher than in the other polypeptide segment (loop 2) contributing to the metal coordination (Fig. 2). Independently of the way that loop 1 contributes to Na^+ coordination, either through anchored water molecules (as in thrombin) or directly (as in FXa), it is the backbone conformation of loop 2 that defines the pivotal metal coordination site. What the Dang and Di Cera's rule does not cover is how the Na^+ site architecture may influence the Na^+ dissociation constants (K_d) and monovalent cation specificity of human coagulation serine proteases. Moreover a different Na^+ site architecture may impact on the degree of activation for each enzyme in the presence or not of other modulators, such as substrate or inhibitor in S1 subsite, Ca^{2+} or an exosite-I ligand. In view of the variability in primary and tertiary structure of loop 1 in sodium activated coagulation proteases, it appears that this loop would furnish the fine tuning necessary to explain the different K_d for Na^+ reported in the literature for these enzymes. In fact, it has been shown that mutations in loop 1 are able to redesign the ionic specificity of thrombin [33,34].

4.2. CaMSA discloses novel features of the molecular recognition and allosteric responses in thrombin and other sodium-activated coagulation enzymes

Our hypothesis that new aspects of the molecular recognition of Na^+ in the water channel and changes

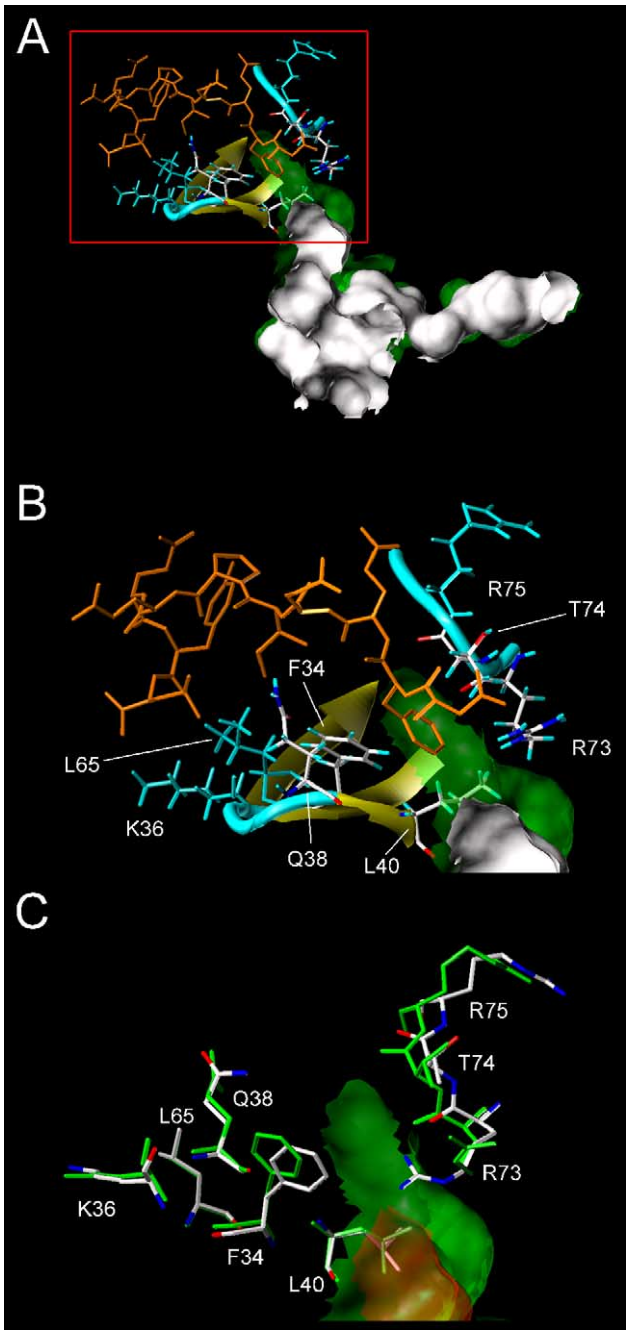

Fig. 8. Analysis of topographical changes responsible for the loss of communication between exosite-I and the active site in thrombin transition to the slow form. A-Mapping of residues in "hot region" next to exosite-I possibly involved in topographical changes upon slow–fast transition in thrombin. Cavity surface for the slow form is shown in solid white over the fast form cavity in transparent green. B-Detail of the red box in A. Residues in the hot region of thrombin fast form making contacts with the modeled exosite-I ligand are shown in sticks. Colored in cyan are general residues, simply making contacts with the exosite-I ligand and in CPK color-scheme are the residues directly involved in disrupting the exosite-I communication upon thrombin transition to the slow form. C-Conformational changes between residues in the fast (green sticks) and slow (CPK-colored sticks) thrombin forms. Hydrogen atoms were omitted for the sake of clarity.

associated with allosteric enhancement of catalytic rate could be revealed by CaMSA of coagulation serine proteases was supported by the results described in Section 3. Indeed, from the cavities typified in Fig. 3, one major difference can be clearly noted which distinguishes thrombin from the other coagulation serine proteases that are able to bind a sodium ion. Whereas the sodium binding water channel in both slow and fast forms of thrombin opens up on the surface of the enzyme opposite to the S1 subsite, the same channel in FVIIa, FIXa, FXa and aPC closes just before reaching the Na^+ binding site. In the thrombin segment comprising residues 185–187 (K185, P186, D186a, E186b, G186c, K186d and R187) the backbone considerably deviates (maximum distance=3.5 Å) from the path followed by the homologous segment in other coagulation proteases. In this 7-residue segment, aPC lacks three of the thrombin insertions and conserves only a half of the remaining residues (D186a and R187) and all other sodium binding coagulation enzymes behave similarly (Fig. 5). A clear consequence is that the sodium binding site in thrombin is directly accessible to the solvent from both sides of the channel, while for the other enzymes it is not. Hence, the mechanism by which the sodium binding event in FVIIa, FIXa, FXa and aPC can be translated into a catalytic rate enhancement may be different from that operating in thrombin.

Inspection of the structures beneath the channels surfaces revealed that they collapse in the segment equivalent to the region delineated by the R187:D222 salt bridge, which has been postulated as a hallmark of the slow–fast transition in thrombin [20]. Based on the results of site-directed mutagenesis coupled to thermodynamic data this interaction has been claimed to be essential for maintaining the integrity of the channel near the Na^+ binding site. However, as can be perceived from comparison of the panels in Fig. 7, despite of the fast form presenting the most stabilizing salt-bridge, the topography on the sodium binding water channel for the slow as well as the fast forms of thrombin shows no significant alteration. Interestingly, the residues involved in this electrostatic interaction are weakly conserved in other sodium binding coagulation enzymes (Fig. 5). In aPC, D222 is substituted by leucine, which makes hydrophobic contacts with the aliphatic part of the R187 side chain. This interaction could partially substitute the stabilizing effect that the salt bridge has over the water channel in thrombin. R187 in aPC is dislocated 2.7 Å in relation to thrombin (from the Cα positions) pointing out of the channel due to the steric blockage by the isobutyl moiety of the L222 side chain (Fig. 6B). In every FXa structure, the aliphatic part of the side chain of a lysine residue (K223) occupies position equivalent to the isobutyl moiety of L222 in aPC. In order to accommodate the bulkier K222 side chain, FXa seemed to have acquired a compensatory mutation in position 187, the R187Q (thrombin→FXa) substitution. The Q187 side chain being two atoms shorter than R187 frees space for K222 (Fig. 6C). A similar behavior is observed in FIXa and FVIIa structures, where the R187:D222 pair of thrombin is substituted for G187:K222 and G187:V222, respectively. The above analysis raises a question about the requirement of a strong stabilizing interaction between residues in positions 187 and 222 to stabilize the channel structure in coagulation enzymes other than thrombin.

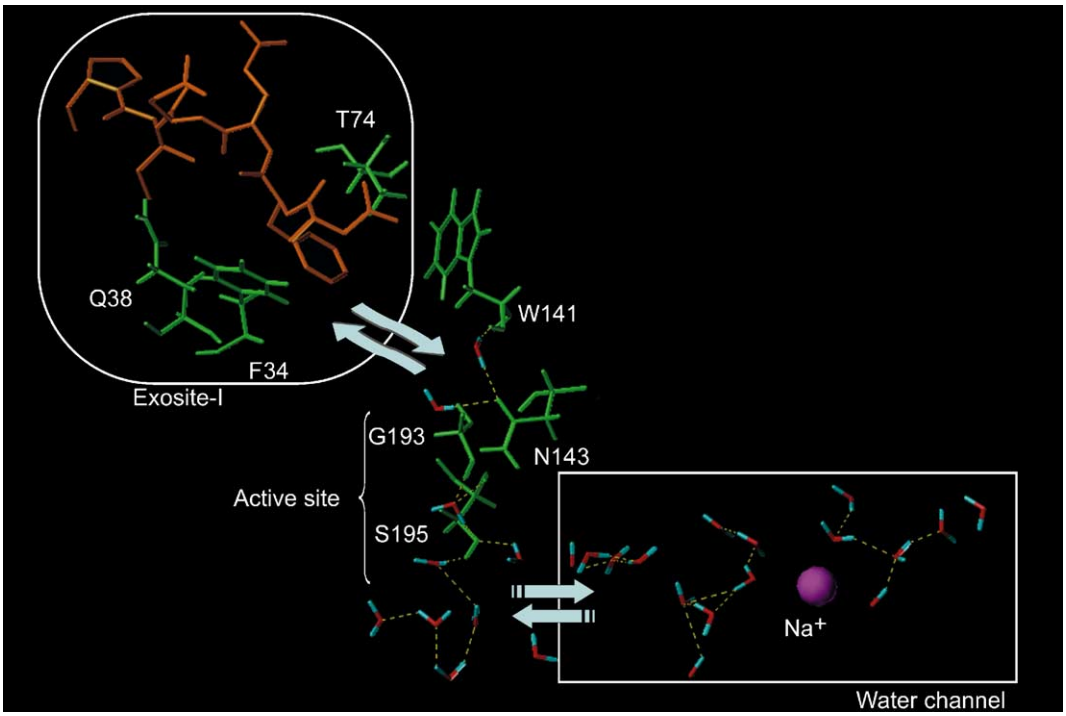

Fig. 9. Proposed structural mechanism for linking conformational changes in the exosite-I to the S1 subsite and adjoining water channel in thrombin. See text for thorough description. For clarity, some of the residues involved in binding the hirugen surrogate, *N*-acetylhirudin[53–64]-Tyr63-sulfate (orange sticks), in exosite-I were omitted (K36, L65, R73 and R75).

Residue D221 belongs to the periphery of the allosteric core in thrombin and fixes one of the water molecules involved in Na^+ coordination in the fast form [20]. It is also a key residue in the allosteric transduction, i.e., in transmitting changes in the sodium binding site to the S1 subsite. In factors VIIa, IXa and Xa, D221 is substituted for Ala whereas in aPC it is mutated to a Gly residue (Fig. 5). In these enzymes, the Asp carboxylate necessary to bind one of the water molecules that coordinate de sodium ion is missing. This indicates that either the water network found in thrombin channel must organize differently in the other coagulation enzymes in order to bind the Na^+ ion or a distinct set of binding partners must be involved in the Na^+ coordination. In support of the later hypothesis, in FXa and aPC, two out of four water molecules coordinating Na^+ in thrombin (waters bound to D221 and Y184a) are replaced by carbonyl groups from residues in loop 1. Noteworthy, the D221X substitutions (thrombin→FVIIa, FIXa, FXa and aPC) are most probably compensatory mutations since they open up space for accommodating the alternative conformation of bulky side chains in position 187.

Other interactions, specific to each enzyme, are found to help in giving structural stabilization to the water channel in the absence of the salt bridge R187:D222 that occurs in thrombin. In aPC, strong hydrogen bonds are found between the guanidinium group of R187 and the G221 carbonyl (2.4 Å $R187^{N-H}$ to $^{O\frown C}G221$) and between the backbones of G186a and L222. In FXa, additional channel stabilization is provided by a hydrogen bond involving the Y225 and H185 side chains.

4.3. Role of position 192 in controlling the access to the S1 subsite entrance

It has been shown that the E192A mutation affects poorly Na^+ affinity and clearly has no impact over thrombin interaction with the synthetic substrate FPR [20]. Nevertheless, a significant rearrangement in E192 side chain has been detected in the original report of thrombin slow and fast forms structures [20]. At the time, it was proposed that E192 would have a role in connecting changes in the Na^+ binding site to the active site through the water network. Indeed, in both thrombin forms, E192 interacts with G142, N143, G193 and C191, but in the fast form E192 is orientated in such manner that it is able to communicate with S195 through a water-mediated hydrogen bonding network (Fig. 7). It is noteworthy that a similar E192 reorientation has been observed in several conditions denoting an inherent flexibility for the side chain of this residue: (i) when sodium binding is disrupted by the D221A/D222K mutations present in the thrombin variant ARK [35]; (ii) upon collapse of the S1 subsite pocket coupled to abrogation of sodium binding and allosteric transduction in the W215A/E217A thrombin mutant [36] and (iii) on PPACK binding to the fast form [20].

Still obscure is why Ala mutation of a residue suffering a major conformational change detected from the comparison of structures standing for thrombin slow and fast forms had no impact on Na^+ binding or allosteric transduction. A possible explanation for this apparent contradiction has been claimed in terms of a strict role for residue E192 in the recognition of larger substrates by thrombin such as Protein C [20]. They

proposed that the rearrangement in E192 side chain upon sodium release would facilitate binding of the anticoagulant (slow) thrombin form to Protein C by minimizing the electrostatic repulsion with the acidic P3 and P3 residues. This hypothesis was recently refuted by results from site-directed thermodynamic analysis showing that E192 does not pertain to the Protein C binding epitope neither in the free-thrombin nor in the thrombomodulin complex [37].

At any rate, the cavity shapes obtained in our analysis clearly depict the influence of the residue in position 192 in the size of the S1 subsite opening in the different coagulation proteases sensitive to sodium binding (Fig. 3). From the alignment in Fig. 5, it was verified that while aPC retained the glutamate in 192, FIXa and FXa had it mutated to Q192. In addition to the loss of the E192 negative charge, Q192 side chain conformation is significantly altered by a modification in $\chi 1$ that results in the relocation of its polar side chain away from the S1 subsite entrance, turning this pocket wider in FXa than in thrombin or aPC. A more drastic mutation in relation to thrombin occurred in FVIIa where E192 was mutated to K192.

4.4. A possible mechanism for the thermodynamic linkage between the exosite-I, S1 subsite and the Na^+ binding site on thrombin

One major aim of our analysis was to extract more data from the available sodium-free and sodium-bound thrombin structures through CaMSA. As mentioned before, a remarkable result from our analysis was that the connection between exosite-I and S1 subsite is lost in thrombin slow form due to topographical changes over the region encompassing the prime-side subsites and exosite-I periphery (Fig. 4). The kinetic mechanism supporting the enhanced catalytic rate of the fast form involves greater diffusion rates of the substrate to the binding cleft in the enzyme and higher acylation rates (reviewed in Ref. [4]). Both features are compatible, respectively, with the greater SAS as provided by the additional surface extending to the exosite-I and with the slight increase in the channel lipophilicity in the sodium bound enzyme (Table 1). The later observation is in line with our previous conclusions about lipophilicity governing binding affinities in the S1 subsite in trypsin-like enzymes [25]. Moreover, changes in lipophilicty may be associated to tiny conformational changes in residues exposed to the surface resulting in lesser exposition of polar residues to the solvent. Such distinct properties of the fast and slow thrombin structures have not been described before.

By carefully inspecting the molecular surfaces and their underlying residues, it was possible to identify a “hot region” as being responsible for the extension of the channel surface to the exosite-I in the Na^+ bound form of thrombin. F34, Q38 and L40 in the region corresponding to the two central β-strands comprising residues 29–36 and 38–47 from the N-terminal β-barrel, and residues R73 and T74 from a loop and a short β-strand that delineate part of the exosite-I constitute this hot region (Fig. 8B). As can be perceived from the superposition of these residues in the ligand-free slow and fast forms depicted in Fig. 8C, upon sodium binding, a significant conformational change in R73 side chain occurs. This promotes the formation of two hydrogen bonding interactions with segment 151–153 in the C-terminal domain of the fast form that culminates in a displacement (RMSD) of 1.92 Å in the position of Q151 side chain.

The hot region responsible for disrupting the surface linkage between S1 subsite and exosite-I in thrombin slow form is located around 25 Å away from the sodium site. Therefore, one should expect to find an intricate set of interactions in thrombin responsible for the long range communication between exosite-I and the sodium binding site. W141, G193 and residues in the segment 151–152 appeared as interesting candidates for playing this role since they are in contact distance (4.0 Å) from residues in the hot region. Residues Q151, P152 and S153 are located at the C-terminal tip of the autolysis loop (141–152), while W141 is situated at the opposite tip. Although the central part of the autolysis loop is usually disordered, these residues act as anchors and present low to average temperature factors. On the other hand, G193 constitutes the oxyanion hole and therefore furnishes a direct communication with the catalytic apparatus, which in turn is linked to the sodium binding water channel through the S1 subsite. Residue W141, in turn, has been implicated in the past in the fluorescence increases that are detected on exosite-I binding by protease-activated receptor (PAR) peptides [38]. Recent experimental data give support to the role of W141 in connecting events in the active site to changes in exosite-I [39]. A series of amide $H/^2H$ studies showed that W141 loses SAS on PPACK binding, which suggests that W141, even though not contacting directly PPACK, may transmit alterations in the active site (and indirectly in the sodium binding site) to the exosite-I, mainly by contacting R73.

Our results combined with literature data permitted us to propose the mechanism delineated in Fig. 9. The Na^+ binding event is thought to be transmitted to the active site S195 through a rearrangement in the water network in the hydrophilic channel adjacent to the S1 subsite [20]. N143 possibly senses such changes in the active site through the oxyanion hole (G193) and passes the information up to W141, in the exosite-I periphery, through water mediated hydrogen bonds. Conformational changes in W141 related to differential solvent exposure are then transmitted to residues in the hot region (F34, Q38, R73 and T74), which in turn, move their side chains toward the cavity and abrogate the continuity on the surface connecting the active site to the exosite-I. Finally, repositioning of residues in the hot region, including K36, L65, T74 and R75 are translated into different binding affinities displayed by the slow form for specific ligands in exosite-I, as hirugen and thrombomodulin.

Considering the above exposition, one further question arises: if residues in the hot region in addition to E192 are important for the topographical changes observed during slow fast transition, so why these residues do not present relevant thermodynamic signatures in thrombin allostery? The case of E192 has been discussed before, but the issue regarding F34,

Q38, R73 and T74 remains obscure. Nevertheless, one could hypothesize that once these residues are located in the exosite-I, in order to detect a clear effect upon Ala mutation, activity assays should be performed with ligands also interacting with this site and not just with the active site like the FPR substrate used before [20]. Indeed, recent site-specific thermodynamic experiments have confirmed this hypothesis by showing that T74 among other thrombin residues (K36, L65 and R75) are responsible for hirudin binding with higher affinity for the fast form [40]. Other residues, such as L40, the 151–153 segment and W141 were not mutated previously [20] and therefore still wait for further experimental data in order to confirm their roles in thrombin allostery. At any rate, a multiple sequence alignment (not shown) reveals a high degree of conservation of residues in the hot region among several thrombin orthologues but not within other chymotrypsin-like serine proteases, giving additional support for their role in the function of thrombin. For instance, R73 is completely conserved from human to hagfish. On the other hand, F34 is strictly conserved on mammalian thrombins, being substituted by a tyrosine in orthologues from other vertebrates like chicken and fishes. Similarly T74 is conserved among mammalian species and zebrafish but is mutated to Ala in other vertebrates.

5. Concluding remarks

We have characterized the structure, topography and lipophilicity of the Na^+ channel in the sole available structure of aPC and in all FVIIa, FIXa and FXa structures available in the PDB. Through application of CaMSA we have unveiled that the pore opening distal to the S1 subsite giving access to the Na^+ binding site in thrombin is unique to this enzyme among other coagulation proteases activated by sodium ion. The shorter loop 1 and the lack of a R187:D222 salt bridge in aPC and factors VIIa, IXa and Xa could be invoked to rationalize the different channel shapes. Such remarkable distinction may have a bearing in the mechanism evolved to acquire affinity for monovalent cations and specificity for Na^+ in coagulation enzymes.

A main goal of our analysis consisted in the comparison of the crystallographic structures representing the thrombin slow and fast forms in the search for obvious differences in the S1 pocket and on the shape and lipophilicity of the water channel that shelters the sodium binding site. From the analysis of molecular surfaces we disclosed previously unobserved conformational changes possibly associated with the slow–fast transition triggered by Na^+ binding in thrombin. These conformational changes are mapped to residues R73, T74, R75 and F34 located in the exosite-I region.

Our general observations and the proposed structural mechanism for linking sites thermodynamically coupled in thrombin surface were supported by both published and unpublished experimental results we were unaware of by the time the analysis was performed [40]. Nevertheless, future work with molecular dynamics simulations of the slow–fast transition in thrombin as well as other sodium-activated coagulation proteases would provide a reasonable test for our conclusions since crystallographic analyses have proved to be insufficient to map the tiny conformational changes involved in this process.

6. Note added in proof

During preparation of the manuscript a paper by Schmidt et al. on the Na^+ site of FIXa was published [41]. Distinctly from us, these authors propose a Na^+ binding site strictly equivalent to that on FXa, aPC and FVIIa. They also effectively show that the FIXa Na^+ site is linked strongly to the S1 and FVIIa binding sites but only weakly to the Ca^{2+} site.

Acknowledgments

This work was supported by CNPq, FAPERJ and PAPES-FIOCRUZ. FPSJr was a CNPq Dsc fellowship recipient. R.B.A. acknowledges a FAPERJ grant (E26-152–174/2002). We thank Dr. E. Di Cera (Washington University School of Medicine, St. Louis) for sharing unpublished results and fruitful discussions.

References

[1] M. Hoffman, Remodeling the blood coagulation cascade, J. Thromb. Thrombolysis 16 (2003) 17–20.
[2] E.W. Davie, K. Fujikawa, W. Kisiel, The coagulation cascade: initiation, maintenance, and regulation, Biochemistry 30 (1991) 10363–10370.
[3] E.W. Davie, A brief historical review of the waterfall/cascade of blood coagulation, J. Biol. Chem. 278 (2003) 50819–50832.
[4] E. Di Cera, Thrombin: a paradigm for enzymes allosterically activated by monovalent cations, C.R. Biol. 327 (2004) 1065–1076.
[5] E. Di Cera, E.R. Guinto, A. Vindigni, Q.D. Dang, Y.M. Ayala, M. Wuyi, A. Tulinsky, The Na^+ binding site of thrombin, J. Biol. Chem. 270 (1995) 22089–22092.
[6] C. Orthner, D.P. Kosow, The effect of metal ions on the amidolytic activity of human factor Xa (activated Stuart–Prower factor), Arch. Biochem. Biophys. 185 (1978) 400–406.
[7] C. Orthner, D.P. Kosow, Evidence that human alpha-thrombin is a monovalent cation-activated enzyme, Arch. Biochem. Biophys. 202 (1980) 63–75.
[8] S.A. Steiner, F.J. Castellino, Kinetic studies of the role of monovalent cations in the amidolytic activity of activated bovine plasma protein C, Biochemistry 21 (1982) 4609–4614.
[9] Q.D. Dang, E. Di Cera, Residue 225 determines the Na(+)-induced allosteric regulation of catalytic activity in serine proteases, Proc. Natl. Acad. Sci. U. S. A. 93 (1996) 10653–10656.
[10] E. Zhang, A. Tulinsky, The molecular environment of the Na^+ binding site of thrombin, Biophys. Chemist. 63 (1997) 185–200.
[11] Q.D. Dang, A. Vindigni, E. Di Cera, An allosteric switch controls the procoagulant and anticoagulant activities of thrombin, Proc. Natl. Acad. Sci. U. S. A. 92 (1995) 5977–5981.
[12] T. Rose, E. Di Cera, Three-dimensional modeling of thrombin–fibrinogen interaction, J. Biol. Chem. 277 (2002) 18875–18880.
[13] A.O. Pineda, A.M. Cantwell, L.A. Bush, T. Rose, E. Di Cera, The thrombin epitope recognizing thrombomodulin is a highly cooperative hot spot in exosite I, J. Biol. Chem. 277 (2002) 32015–32019.
[14] W. Bode, P. Schwager, The single calcium-binding site of crystalline bovin beta-trypsin, FEBS Lett. 56 (1975) 139–143.
[15] A.R. Rezaie, T. Mather, F. Sussman, C.T. Esmon, Mutation of Glu-80→Lys results in a protein C mutant that no longer requires Ca^{2+} for rapid activation by the thrombin–thrombomodulin complex, J. Biol. Chem. 269 (1994) 3151–3154.
[16] W.G. Owen, C.T. Esmon, Functional properties of an endothelial cell cofactor for thrombin-catalyzed activation of protein C, J. Biol. Chem. 256 (1981) 5532–5535.

[17] P. Wildgoose, D. Foster, J. Schiodt, F.C. Wiberg, J.J. Birktoft, L.C. Petersen, Identification of a calcium binding site in the protease domain of human blood coagulation factor VII: evidence for its role in factor VII-tissue factor interaction, Biochemistry 32 (1993) 114–119.
[18] A.R. Rezaie, C.T. Esmon, Asp-70→Lys mutant of factor X lacks high affinity Ca^{2+} binding site yet retains function, J. Biol. Chem. 269 (1994) 21495–21499.
[19] A.O. Pineda, C.J. Carrell, L.A. Bush, S. Prasad, S. Caccia, Z.W. Chen, F.S. Mathews, E. Di Cera, Molecular dissection of Na^{+} binding to thrombin, J. Biol. Chem. 279 (2004) 31842–31853.
[20] A.O. Pineda, C.J. Carrel, L.A. Bush, S. Prasad, S. Caccia, Z.W. Chen, F.S. Mathews, E. Di Cera, Molecular dissection of Na^{+} binding to thrombin, J. Biol. Chem. 279 (2004) 31842–31853.
[21] M.T. Lai, E. Di Cera, J.A. Shafer, Kinetic pathway for the slow to fast transition of thrombin. Evidence of linked ligand binding at structurally distinct domains, J. Biol. Chem. 272 (1997) 30275–30282.
[22] A.E. Schmidt, K. Padmanabhan, M.C. Underwood, W. Bode, T. Mather, S.P. Bajaj, Thermodynamic linkage between the S1 site, the Na^{+} site, and the Ca^{2+} site in the protease domain of human activated protein C (APC). Sodium ion in the APC crystal structure is coordinated to four carbonyl groups from two separate loops, J. Biol. Chem. 277 (2002) 28987–28995.
[23] M.C. Underwood, D. Zhong, A. Mathur, T. Heyduk, S.P. Bajaj, Thermodynamic linkage between the S1 site, the Na^{+} site, and the Ca^{2+} site in the protease domain of human coagulation factor Xa. Studies on catalytic efficiency and inhibitor binding, J. Biol. Chem. 275 (2000) 36876–36884.
[24] A.E. Schmidt, J.E. Stewart, S.P. Bajaj, Functional linkage between the Na^{+} site, substrate site, and the Ca^{2+} site in the protease domain of human factor IXa (FIXa), Blood 102 (2003) 1074.
[25] F.P. Silva Jr., S.G. De Simone, S1 subsite in snake venom thrombin-like enzymes: can S1 subsite lipophilicity be used to sort binding affinities of trypsin-like enzymes to small-molecule inhibitors? Bioorg. Med. Chem. 12 (2004) 2571–2587.
[26] H.-J. Böhm, G. Schneider, R. Mannhold, et al., (Eds.), Protein–Ligand Interactions: From Molecular Recognition to Drug Design, Wiley–VCH Gmbh and Co. KGaA, Weinheim, 2003.
[27] M. Nayal, E. Di Cera, Valence screening of water in protein crystals reveals potential Na^{+} binding sites, J. Mol. Biol. 256 (1996) 228–234.
[28] M.L. Connolly, Solvent-accessible surfaces of proteins and nucleic acids, Science 221 (1983) 709–713.
[29] J.S. Delaney, Finding and filling protein cavities using cellular logic operations, J. Mol. Graph. 10 (1992) 174–177.
[30] T.E. Exner, M. Keil, G. Moeckel, J. Brickmann, Identification of substrate channels and protein cavities, J. Mol. Mod. 4 (1998) 340–343.
[31] A. Ghose, G. Crippen, Atomic physicochemical parameters for three-dimensional structure-directed quantitative structure–activity relationships I. Partition coefficients as a measure of hydrophobicity, J. Comput. Chem. 7 (1986) 565–577.
[32] A. Wei, R.S. Alexander, J. Duke, H. Ross, S.A. Rosenfeld, C.H. Chang, Unexpected binding mode of tick anticoagulant peptide complexed to bovine factor Xa, J. Mol. Biol. 283 (1998) 147–154.
[33] S. Prasad, K.J. Wright, D.B., L.A. Bush, A.M. Cantwell, E. Di Cera, Redesigning the monovalent cation specificity of an enzyme, Proc. Natl. Acad. Sci. U. S. A. 100 (2003) 13785–13790.
[34] S. Prasad, A.M. Cantwell, L.A. Bush, P. Shih, H. Xu, E. Di Cera, Residue Asp-189 controls both substrate binding and the monovalent cation specificity of thrombin, J. Biol. Chem. 279 (2004) 10103–10108.
[35] A.O. Pineda, E. Zhang, E.R. Guinto, et al., Crystal structure of the Thrombin mutant D221A/D222K: the Asp222:Arg187 ion-pair stabilizes the fast form, Biophys. Chemist. 112 (2004) 253–256.
[36] A.O. Pineda, Z.-W. Chen, S. Caccia, A.M. Cantwell, S.N. Savvides, G. Waksman, F.S. Mathews, E. Di Cera, The anticoagulant thrombin mutant W215A/E217A has a collapsed primary specificity pocket, J. Biol. Chem. 279 (2004) 39824–39828.
[37] H. Xu, L.A. Bush, A.O. Pineda, S. Caccia, E. Di Cera, Thrombomodulin changes the molecular surface of interaction and the rate of complex formation between thrombin and protein C, J. Biol. Chem. 280 (2005) 7956–7961.
[38] M.M. Krem, E. Di Cera, Dissecting substrate recognition by thrombin using the inactive mutant S195A, Biophys. Chemist. 100 (2003) 315–323.
[39] C.H. Croy, J.R. Koeppe, S. Bergqvist, E.A. Comives, Allosteric changes in solvent accessibility observed in thrombin upon active site occupation, Biochemistry 43 (2004) 5246–5255.
[40] K.E. Mengwasser, L.A. Bush, P. Shih, A.M. Cantwell, E. Di Cera, Hirudin binding reveals key determinants of thrombin allostery, J. Biol. Chem. 280 (2005) 26997–27003.
[41] A.E. Schmidt, J.E. Stewart, A. Mathur, S. Krishnaswamy, S.P. Bajaj, Na^{+} site in blood coagulation factor IXa: effect on catalysis and factor VIIIa binding, J. Mol. Biol. 350 (2005) 78–91.